

Directional Geometry and Anisotropy in the Partition Graph

Fedor B. Lyudogovskiy

Abstract

We develop a directional formalism for the partition graph G_n based on several canonical reference sets: the main chain, the self-conjugate axis, the spine, and the boundary framework. For each such set S , the graph distance d_S induces a shell structure and a local trichotomy of edges into inward, outward, and level classes. Passing from edges to paths, we define directional corridors as monotone inward geodesics toward a chosen reference set and prove that every vertex admits at least one.

We then prove a structural non-equivalence theorem: for connected G_n , two nonempty reference sets induce the same edgewise directional field if and only if the difference of their distance functions is constant; in particular, distinct reference sets induce distinct directional fields. This provides a first precise formalization of anisotropy in G_n . We also show that every bounded neighborhood of a reference set is accessible by a monotone inward corridor, which gives a directional interpretation to previously established controlled regions around the axis, the spine, and the framework.

Finally, we complement the strict theory with a computational atlas illustrating edgewise directional statistics, directional mixing, local invariant drift, and corridor-based transport profiles.

Keywords: partition graph; integer partitions; directional geometry; anisotropy; graph distance; monotone geodesics; self-conjugate axis; spine; boundary framework; controlled neighborhoods
MSC 2020: 05C12, 05C75, 05A17

1 Introduction

The partition graph G_n is the graph whose vertices are the integer partitions of n and whose edges correspond to elementary unit transfers between parts, followed by reordering into nonincreasing form; see Section 2 for a precise definition. In the preceding papers of this series, several geometric structures have been identified in G_n : the main chain, the self-conjugate axis, central neighborhoods, simplex layers, the degree landscape, the spine, the boundary framework, and rear morphology [5, 6, 7, 8]. A persistent informal theme behind these constructions is that G_n is not isotropic. Certain directions or transport regimes appear to be privileged, while others play visibly different roles.

The aim of this paper is to formalize that intuition. We do not seek a global geometric classification, nor do we attempt to reduce all motion in G_n to a single dominant field. Instead, we develop a strict directional language relative to several canonical reference sets already present in the morphology of G_n : the main chain M_n , the self-conjugate axis Ax_n , the spine Sp_n , and the boundary framework Fr_n . For each such set S , the graph distance d_S produces a shell decomposition of G_n and a local trichotomy of edges into inward, outward, and level classes. Passing from edges to paths, we define directional corridors as monotone inward geodesics toward a chosen reference set.

At the formal level, the paper has three main structural components. First, relative to any nonempty reference set $S \subseteq V(G_n)$, the distance function d_S induces a local trichotomy of edges and a corresponding shell decomposition of G_n . Second, every vertex admits an S -monotone inward geodesic to S , which provides a pathwise notion of directional corridor. Third, if G_n is connected, two nonempty reference sets induce the same edgewise directional field if and

only if the difference of their distance functions is constant; in particular, distinct reference sets induce distinct directional fields. Together with the controlled-access principle for bounded neighborhoods, these results yield a first strict framework for directional geometry and anisotropy in the partition graph.

The contribution of the paper is therefore conceptual and organizational rather than enumerative. The relevant background comes from the global homotopy-theoretic study of $\text{Cl}(G_n)$ and from the companion papers on local morphology, large-scale morphology, axial morphology, simplex stratification, and the degree landscape [3, 4, 5, 6, 7, 8]. The present paper does not re-establish those results; rather, it studies the directional relations among these structures. In particular, once a distinguished region is known to lie in a bounded neighborhood of the axis, the spine, or the framework [6, 5], the corridor formalism immediately converts that containment statement into a directional-access statement. This is the main bridge between the present work and the earlier morphology papers.

We also include a compact computational atlas for the tested range $8 \leq n \leq 12$. The strict theory developed in Sections 2–5 already implies that different reference sets define different directional fields, but it does not by itself quantify the resulting anisotropy. The computations therefore serve two auxiliary purposes: they make the shell geometry visually explicit, and they measure how different directional regimes interact with local invariants such as degree, local simplex dimension, support size, and height.

The paper is organized as follows. Section 2 fixes the canonical reference sets and the basic distance observables. Section 3 introduces edgewise directional classes and the shell-based trichotomy. Section 4 passes from edges to paths and establishes the existence of monotone inward geodesics, which we call directional corridors. Section 5 contains the main structural anisotropy result and the controlled-access principle for bounded neighborhoods. Section 6 presents a computational directional atlas for the tested range $8 \leq n \leq 12$. The final section summarizes the resulting picture and formulates several open problems.

2 Canonical reference sets and directional observables

We now recall the objects that will serve as reference sets in the present paper. Let $V(G_n)$ denote the set of partitions of n written in nonincreasing form. For standard background on integer partitions and Ferrers diagrams, see Andrews and Stanley [1, 2].

Definition 2.1. Let $\lambda = (\lambda_1, \dots, \lambda_k) \vdash n$. Choose two distinct indices i, j with $1 \leq i, j \leq k$ and $\lambda_j > 0$. Replace λ_i by $\lambda_i + 1$ and λ_j by $\lambda_j - 1$, delete the latter if it becomes 0, and reorder the resulting parts into nonincreasing form. If the resulting partition is $\mu \neq \lambda$, we say that μ is obtained from λ by an *elementary unit transfer*.

Two partitions $\lambda, \mu \vdash n$ are adjacent in G_n if one is obtained from the other by a single elementary unit transfer.

This is the same adjacency convention used throughout the earlier papers of the series; in particular, it is the convention underlying the local transfer language and the height function [3, 4].

2.1 Canonical reference sets

The *main chain* is the hook chain

$$M_n = \{(n - k, 1^k) : 0 \leq k \leq n - 1\},$$

joining the two antennas (n) and (1^n) .

The *self-conjugate axis* is

$$\text{Ax}_n = \{\lambda \vdash n : \lambda = \lambda'\}.$$

For the *boundary framework*, we use, following the large-scale morphology paper [5],

$$\text{Fr}_n = M_n \cup L_n \cup R_n,$$

where

$$L_n = \{(n - k, k) : 1 \leq k \leq \lfloor n/2 \rfloor\}$$

is the left edge and $R_n = L'_n$ is its conjugate right edge.

The *spine* Sp_n is taken in the thin sense defined in the axial-morphology paper [6]. Write the self-conjugate partitions of n in decreasing lexicographic order as

$$\sigma_1, \sigma_2, \dots, \sigma_m.$$

For each consecutive pair (σ_i, σ_{i+1}) , choose a shortest path in G_n connecting them that is lexicographically minimal among all such shortest paths. The spine Sp_n is the union of Ax_n with all vertices lying on these chosen paths. This choice is not claimed to be the only reasonable one, but it is sufficiently canonical for the present directional theory and for the computations in Section 6.

2.2 Distance observables, shells, and neighborhoods

Let $S \subseteq V(G_n)$ be nonempty. We write

$$d_S(\lambda) = \min_{\sigma \in S} d_{G_n}(\lambda, \sigma)$$

for the graph distance from λ to S .

For the four canonical reference sets we use the shorthand notation

$$d_M, \quad d_{\text{Ax}}, \quad d_{\text{Sp}}, \quad d_{\text{Fr}}.$$

Definition 2.2. Let $S \subseteq V(G_n)$ be nonempty and let $r \geq 0$. The r -th shell around S is

$$\text{Sh}_S^{(r)} = \{\lambda \in V(G_n) : d_S(\lambda) = r\},$$

and the closed r -neighborhood of S is

$$N_S^{(\leq r)} = \{\lambda \in V(G_n) : d_S(\lambda) \leq r\}.$$

We also use the height function

$$h(\lambda) = \sum_{i \geq 1} i \lambda_i$$

and the support size

$$s(\lambda) = \ell(\lambda),$$

that is, the number of positive parts of λ . These observables already play an important role in the local and degree-theoretic morphology of G_n [4, 8], and they will reappear in Section 6 as part of the directional drift profile.

Remark 2.3. The present paper uses *relative* directional language. There is no absolute notion of inward motion. Instead, we speak about motion toward M_n , Ax_n , Sp_n , or Fr_n , depending on which distance observable is being used.

2.3 Connectivity

The directional-equivalence theorem in Section 5 relies on the fact that G_n is connected.

Proposition 2.4. *For every $n \geq 1$, the partition graph G_n is connected.*

Proof. Let $\lambda = (\lambda_1, \dots, \lambda_k) \vdash n$, with $\lambda_1 \geq \dots \geq \lambda_k > 0$. If $k = 1$, then $\lambda = (n)$.

Assume $k \geq 2$. Choose the smallest part λ_k , and move its units one by one to the largest part λ_1 . Each such step is an elementary unit transfer between two parts, followed by reordering, and therefore corresponds to an edge of G_n . After λ_k transfers, the smallest part disappears, so the number of parts decreases by 1.

Repeating the procedure, we eventually reach the one-part partition (n) . Thus every vertex is connected to (n) , and G_n is connected. \square

3 Directional classes of moves

We now formalize direction at the level of individual edges of G_n .

3.1 Edgewise direction relative to a reference set

Proposition 3.1. *Let $S \subseteq V(G_n)$ be nonempty, and let $\lambda \sim \mu$ in G_n . Then*

$$|d_S(\lambda) - d_S(\mu)| \leq 1.$$

Equivalently, exactly one of the following three cases holds:

$$d_S(\mu) = d_S(\lambda) - 1, \quad d_S(\mu) = d_S(\lambda), \quad d_S(\mu) = d_S(\lambda) + 1.$$

Proof. Choose $\sigma \in S$ such that $d_S(\lambda) = d(\lambda, \sigma)$. Since $\lambda \sim \mu$,

$$d(\mu, \sigma) \leq d(\lambda, \sigma) + 1 = d_S(\lambda) + 1,$$

hence

$$d_S(\mu) \leq d_S(\lambda) + 1.$$

By symmetry,

$$d_S(\lambda) \leq d_S(\mu) + 1.$$

Therefore $|d_S(\lambda) - d_S(\mu)| \leq 1$. \square

Definition 3.2. Let $S \subseteq V(G_n)$ be nonempty, and let $\lambda \sim \mu$.

(i) The edge $\lambda\mu$ is *S-inward* at λ if

$$d_S(\mu) = d_S(\lambda) - 1.$$

(ii) It is *S-outward* at λ if

$$d_S(\mu) = d_S(\lambda) + 1.$$

(iii) It is *S-level* at λ if

$$d_S(\mu) = d_S(\lambda).$$

Corollary 3.3. *Let*

$$\text{Sh}_S^{(r)} = \{\lambda \in V(G_n) : d_S(\lambda) = r\}.$$

Then every edge of G_n either lies inside a single shell $\text{Sh}_S^{(r)}$ or joins two adjacent shells $\text{Sh}_S^{(r)}$ and $\text{Sh}_S^{(r+1)}$.

Proof. Immediate from Proposition 3.1. \square

3.2 Tangential and transverse motion

Definition 3.4. Let $S \subseteq V(G_n)$ be nonempty.

- (i) An edge $\lambda\mu$ is *internal to S* if $\lambda, \mu \in S$.
- (ii) It is *transverse to the S -shell structure* if $d_S(\lambda) \neq d_S(\mu)$.
- (iii) It is *tangential to the S -shell structure* if $d_S(\lambda) = d_S(\mu)$.

Proposition 3.5. Let $S \subseteq V(G_n)$ be nonempty.

- (i) Every edge internal to S is S -level.
- (ii) Every S -inward or S -outward edge is transverse to the S -shell structure.
- (iii) Every S -level edge is tangential to the S -shell structure.

Proof. For (i), if $\lambda, \mu \in S$, then $d_S(\lambda) = d_S(\mu) = 0$, so the edge is S -level. Statements (ii) and (iii) are immediate from the definitions. \square

Remark 3.6. Tangential motion and internal motion should not be conflated. An edge can be tangential to the S -shell structure without being internal to S . For instance, this occurs when both endpoints lie in the same positive shell $\text{Sh}_S^{(r)}$ with $r > 0$.

3.3 Named directional classes and combined signatures

We shall speak of *axial*, *spinal*, *chain*, and *framework* inward/outward/level motion according to whether S equals Ax_n , Sp_n , M_n , or Fr_n .

It is convenient to record several directional fields simultaneously.

Definition 3.7. For an oriented edge (λ, μ) , define the combined directional signature

$$\Sigma(\lambda, \mu) = (\sigma_M(\lambda, \mu), \sigma_{\text{Ax}}(\lambda, \mu), \sigma_{\text{Sp}}(\lambda, \mu), \sigma_{\text{Fr}}(\lambda, \mu)),$$

where

$$\sigma_S(\lambda, \mu) = d_S(\mu) - d_S(\lambda) \in \{-1, 0, +1\}.$$

Definition 3.8. An oriented edge is *directionally coherent* if all nonzero components of its combined directional signature have the same sign. Otherwise it is called *directionally mixed*.

Remark 3.9. The same edge may be inward relative to one reference set, level relative to another, and outward relative to a third. This already shows that the directional geometry of G_n is not governed by a single field.

4 Monotone paths and directional corridors

The edgewise language of Section 3 gives rise to a natural path geometry relative to any chosen reference set S .

4.1 Monotone paths

Definition 4.1. A path

$$P = (\lambda_0, \lambda_1, \dots, \lambda_m)$$

in G_n is called

(i) *S-monotone inward* if

$$d_S(\lambda_{i+1}) = d_S(\lambda_i) - 1 \quad (0 \leq i < m);$$

(ii) *S-monotone outward* if

$$d_S(\lambda_{i+1}) = d_S(\lambda_i) + 1 \quad (0 \leq i < m);$$

(iii) *S-level* if

$$d_S(\lambda_{i+1}) = d_S(\lambda_i) \quad (0 \leq i < m).$$

Lemma 4.2. Let

$$P = (\lambda_0, \lambda_1, \dots, \lambda_m)$$

be an *S-monotone inward path*. Then

$$d_S(\lambda_i) = d_S(\lambda_0) - i \quad (0 \leq i \leq m).$$

In particular,

$$m \leq d_S(\lambda_0).$$

If moreover $\lambda_m \in S$, then

$$m = d_S(\lambda_0),$$

and the path is a geodesic from λ_0 to S .

Proof. The identity follows by induction on i . Since distances are nonnegative, $d_S(\lambda_0) - i \geq 0$, so $i \leq d_S(\lambda_0)$ for all i , and in particular $m \leq d_S(\lambda_0)$. If $\lambda_m \in S$, then $d_S(\lambda_m) = 0$, so $0 = d_S(\lambda_0) - m$, hence $m = d_S(\lambda_0)$. No path from λ_0 to S can have length smaller than $d_S(\lambda_0)$. \square

Lemma 4.3. Let $\lambda \in V(G_n)$ with $d_S(\lambda) > 0$. Then λ has a neighbor μ such that

$$d_S(\mu) = d_S(\lambda) - 1.$$

Proof. Choose $\sigma \in S$ such that $d(\lambda, \sigma) = d_S(\lambda)$, and let

$$\lambda = \lambda_0, \lambda_1, \dots, \lambda_r = \sigma$$

be a shortest path from λ to σ , where $r = d_S(\lambda)$. Then λ_1 is adjacent to λ , and

$$d_S(\lambda_1) \leq d(\lambda_1, \sigma) = r - 1 = d_S(\lambda) - 1.$$

By Proposition 3.1,

$$d_S(\lambda_1) \geq d_S(\lambda) - 1.$$

Hence $d_S(\lambda_1) = d_S(\lambda) - 1$. \square

Proposition 4.4. For every vertex $\lambda \in V(G_n)$, there exists an *S-monotone inward path* from λ to S of length $d_S(\lambda)$. Equivalently, every vertex admits an *S-monotone inward geodesic* to S .

Proof. If $d_S(\lambda) = 0$, there is nothing to prove. Otherwise Lemma 4.3 gives a neighbor λ_1 with $d_S(\lambda_1) = d_S(\lambda) - 1$. Repeating the argument inductively yields a path

$$\lambda = \lambda_0, \lambda_1, \dots, \lambda_r$$

such that

$$d_S(\lambda_i) = d_S(\lambda) - i \quad (0 \leq i \leq r).$$

The process stops when $d_S(\lambda_r) = 0$, that is, when $\lambda_r \in S$. Then $r = d_S(\lambda)$, and Lemma 4.2 shows that the path is geodesic. \square

Corollary 4.5. *Let*

$$P = (\lambda_0, \lambda_1, \dots, \lambda_r)$$

be any path from λ_0 to a vertex of S of length $r = d_S(\lambda_0)$. Then P is S -monotone inward.

Proof. Since P has length $d_S(\lambda_0)$ and ends in S , it is a geodesic from λ_0 to S . For each i we have

$$d_S(\lambda_i) \leq r - i,$$

because the tail

$$\lambda_i, \lambda_{i+1}, \dots, \lambda_r$$

connects λ_i to S in $r - i$ steps. On the other hand, the initial segment

$$\lambda_0, \lambda_1, \dots, \lambda_i$$

has length i , so

$$d_S(\lambda_0) \leq i + d_S(\lambda_i).$$

Since $r = d_S(\lambda_0)$, it follows that

$$r \leq i + d_S(\lambda_i),$$

and hence

$$d_S(\lambda_i) = r - i \quad (0 \leq i \leq r).$$

Therefore

$$d_S(\lambda_{i+1}) = d_S(\lambda_i) - 1 \quad (0 \leq i < r),$$

so P is S -monotone inward. \square

4.2 Directional corridors and pathwise transport

Definition 4.6. An S -directional corridor is an S -monotone inward geodesic. In particular, we speak of axial, spinal, chain, and framework corridors when $S = \text{Ax}_n, \text{Sp}_n, M_n,$ and $\text{Fr}_n,$ respectively.

Remark 4.7. No uniqueness is claimed. A given vertex may admit many different directional corridors to the same reference set.

Definition 4.8. Let $P = (\lambda_0, \dots, \lambda_m)$ be a path in G_n .

- (i) P is *internal* to S if $\lambda_i \in S$ for all i ;
- (ii) P is *shell-tangential* with respect to S if it is S -level;
- (iii) P is *shell-transverse* with respect to S if every edge of P is S -inward or S -outward.

Proposition 4.9. *Let P be a path in G_n .*

- (i) *If P is internal to S , then P is S -level.*

(ii) Every S -directional corridor is shell-transverse with respect to S .

Proof. If every vertex of P belongs to S , then every vertex has $d_S = 0$, so every edge is S -level. If P is an S -directional corridor, then every edge is S -inward by definition. \square

Remark 4.10. An S -level path need not be internal to S . This happens whenever some positive shell $\text{Sh}_S^{(r)}$, $r > 0$, contains a nontrivial path.

5 Anisotropy and interaction with established morphology

The results of this section isolate a basic strict form of anisotropy in G_n .

5.1 Height orientation

Lemma 5.1. *If $\lambda \sim \mu$ in G_n , then*

$$h(\lambda) \neq h(\mu).$$

In particular, every edge of G_n admits a unique height direction.

Proof. By definition of the partition graph, adjacent vertices differ by a single elementary unit transfer between two parts, followed by reordering into nonincreasing form. Let μ be obtained from λ by transferring one unit from the j -th part to the i -th part before reordering, where $i \neq j$.

For any partition $\xi = (\xi_1, \xi_2, \dots)$, write

$$T_r(\xi) := \sum_{t \geq r} \xi_t.$$

Then

$$h(\xi) = \sum_{r \geq 1} T_r(\xi),$$

since

$$\sum_{r \geq 1} T_r(\xi) = \sum_{r \geq 1} \sum_{t \geq r} \xi_t = \sum_{t \geq 1} t \xi_t.$$

Assume first that $i < j$. Before reordering, the modified sequence has the same total sum as λ , and its partial sums are larger than those of λ for $k = i, \dots, j - 1$ and unchanged otherwise. After reordering into nonincreasing form, the sums of the first k terms can only increase. Hence

$$\sum_{t=1}^k \mu_t \geq \sum_{t=1}^k \lambda_t \quad (k \geq 1),$$

with strict inequality for some k . Since $|\lambda| = |\mu|$, this is equivalent to

$$T_r(\mu) \leq T_r(\lambda) \quad (r \geq 1),$$

with strict inequality for some r . Therefore

$$h(\mu) = \sum_{r \geq 1} T_r(\mu) < \sum_{r \geq 1} T_r(\lambda) = h(\lambda).$$

The case $i > j$ is symmetric, and yields $h(\mu) > h(\lambda)$. In either case,

$$h(\lambda) \neq h(\mu).$$

Thus adjacent vertices always have distinct heights. \square

Proposition 5.2. *Orient each edge of G_n from the endpoint of smaller height to the endpoint of larger height. Then the resulting orientation is acyclic.*

Proof. By Lemma 5.1, this orientation is well defined on every edge. Along every oriented edge the height strictly increases. Therefore a directed cycle would force

$$h(\lambda_0) < h(\lambda_1) < \cdots < h(\lambda_k) = h(\lambda_0),$$

which is impossible. □

Remark 5.3. The height orientation is intrinsic: it does not depend on a chosen reference set. It should therefore be compared with the shell-based directional fields rather than identified with any one of them.

5.2 Directional equivalence and its failure

Definition 5.4. Let $S, T \subseteq V(G_n)$ be nonempty. We say that S and T are *directionally equivalent* if

$$\sigma_S(\lambda, \mu) = \sigma_T(\lambda, \mu)$$

for every oriented edge (λ, μ) of G_n .

Theorem 5.5. *Assume that G_n is connected. Let $S, T \subseteq V(G_n)$ be nonempty. Then the following are equivalent:*

(i) S and T are directionally equivalent;

(ii) the function

$$d_S - d_T$$

is constant on $V(G_n)$.

Proof. If $d_S - d_T$ is constant, then for every oriented edge (λ, μ) ,

$$d_S(\mu) - d_S(\lambda) = d_T(\mu) - d_T(\lambda),$$

so S and T are directionally equivalent.

Conversely, assume that $\sigma_S(\lambda, \mu) = \sigma_T(\lambda, \mu)$ for every oriented edge. Fix a base vertex $\lambda_0 \in V(G_n)$ and let $\lambda \in V(G_n)$ be arbitrary. Since G_n is connected by Proposition 2.4, there exists a path

$$\lambda_0, \lambda_1, \dots, \lambda_m = \lambda.$$

Summing the edge increments along this path yields

$$d_S(\lambda) - d_S(\lambda_0) = \sum_{i=0}^{m-1} \sigma_S(\lambda_i, \lambda_{i+1}) = \sum_{i=0}^{m-1} \sigma_T(\lambda_i, \lambda_{i+1}) = d_T(\lambda) - d_T(\lambda_0).$$

Hence

$$d_S(\lambda) - d_T(\lambda) = d_S(\lambda_0) - d_T(\lambda_0),$$

which is independent of λ . □

Corollary 5.6. *Let $S, T \subseteq V(G_n)$ be nonempty and distinct. Then S and T are not directionally equivalent. Equivalently, there exists an oriented edge (λ, μ) such that*

$$\sigma_S(\lambda, \mu) \neq \sigma_T(\lambda, \mu).$$

Proof. Suppose that S and T are directionally equivalent. By Theorem 5.5, the function

$$d_S - d_T$$

is constant on $V(G_n)$; write this constant as c .

Choose $s \in S$ and $t \in T$. Since $d_S(s) = 0$ and $d_T(t) = 0$, we have

$$c = d_S(s) - d_T(s) = -d_T(s) \leq 0$$

and

$$c = d_S(t) - d_T(t) = d_S(t) \geq 0.$$

Hence $c = 0$, so

$$d_S = d_T$$

on all of $V(G_n)$.

Now let $s \in S$. Then $d_S(s) = 0$, hence $d_T(s) = 0$, which means that $s \in T$. Thus $S \subseteq T$. By symmetry, $T \subseteq S$. Therefore $S = T$, contradicting the assumption that the two sets are distinct. \square

Remark 5.7. Applying Corollary 5.6 to

$$M_n, \quad \text{Ax}_n, \quad \text{Sp}_n, \quad \text{Fr}_n,$$

we conclude that the four canonical directional fields are pairwise distinct. This is the basic strict form of anisotropy in G_n .

5.3 Access to bounded neighborhoods

The corridor formalism extends from reference sets to their bounded neighborhoods.

Proposition 5.8. *Let $S \subseteq V(G_n)$ be nonempty, and let $r \geq 0$. For every vertex $\lambda \in V(G_n)$, there exists a path from λ to the closed neighborhood*

$$N_S^{(\leq r)} = \{\mu \in V(G_n) : d_S(\mu) \leq r\}$$

which is S -monotone inward and has length

$$\max\{d_S(\lambda) - r, 0\}.$$

In particular, if $d_S(\lambda) \geq r$, then there exists an S -monotone inward geodesic from λ to $N_S^{(\leq r)}$ of length $d_S(\lambda) - r$.

Proof. If $d_S(\lambda) \leq r$, the trivial path suffices. Otherwise choose an S -directional corridor

$$\lambda = \lambda_0, \lambda_1, \dots, \lambda_m$$

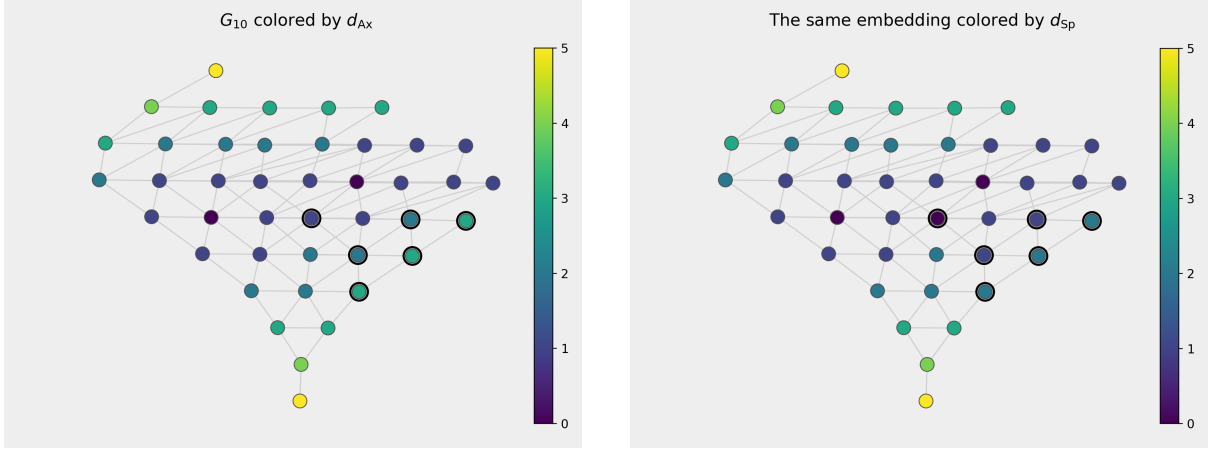
from λ to S , where $m = d_S(\lambda)$ by Proposition 4.4. By Lemma 4.2,

$$d_S(\lambda_i) = d_S(\lambda) - i.$$

Setting $i_* = d_S(\lambda) - r$, we obtain $d_S(\lambda_{i_*}) = r$, so $\lambda_{i_*} \in N_S^{(\leq r)}$. The initial segment of the corridor has length $d_S(\lambda) - r$ and is optimal, since each edge changes d_S by at most 1. \square

Definition 5.9. A set $X \subseteq V(G_n)$ is S -controlled with radius r if

$$X \subseteq N_S^{(\leq r)}.$$



(a) Coloring by d_{Ax} ; black rings mark vertices where $d_{Ax} \neq d_{Sp}$.

(b) Coloring by d_{Sp} ; black rings mark vertices where $d_{Ax} \neq d_{Sp}$.

Figure 1: Two shell structures on the same embedding of G_{10} , shown with identical vertex positions to isolate the difference between axial and spinal shells. The two shell structures are close but not identical; vertices where the two shell distances differ are marked by black rings.

Proposition 5.10. *Let $X \subseteq V(G_n)$ be S -controlled with radius r . Then every vertex $\lambda \in V(G_n)$ admits an S -monotone inward geodesic to the controlled region $N_S^{r(\leq r)}$. If $d_S(\lambda) \geq r$, the length of such a geodesic is $d_S(\lambda) - r$.*

Proof. Immediate from Proposition 5.8. □

Remark 5.11. Proposition 5.10 is intentionally formulated in abstract form. Its role is to convert previously established containment statements into directional ones. Whenever a distinguished family of vertices is already known to lie in a bounded neighborhood of Ax_n , Sp_n , or Fr_n , the proposition immediately yields corresponding axial, spinal, or framework corridors to that region.

6 Computational directional atlas

We now complement the strict theory with a small computational atlas. All computations in this section were carried out for the tested range $8 \leq n \leq 12$. The figures use fixed layouts for G_{10} and G_{12} , while the tables summarize either selected values of n or the whole tested range.

For each n , we enumerated all partitions of n , constructed the graph G_n using Definition 2.1, and computed the reference sets M_n , Ax_n , Sp_n , and Fr_n . We then computed the distance fields d_M , d_{Ax} , d_{Sp} , and d_{Fr} . Local degrees are graph degrees. The local simplex dimension of a vertex was computed as the maximal clique size containing that vertex minus one. Canonical directional corridors were obtained by choosing, at each step, the lexicographically smallest neighbor that decreases the relevant distance by one.

6.1 Edgewise directional statistics

Figures 1a and 1b show the vertex shell geometry of G_{10} relative to the axis and the spine, using the same embedding in both panels. The two shell structures are very close for G_{10} , so the vertices at which d_{Ax} and d_{Sp} differ are marked by black rings. Figures 2a and 2b display the corresponding same-shell versus cross-shell edge behavior.

Observation 6.1. In the tested range, the shell geometry around the canonical reference sets is visibly non-uniform. In particular, the level/transverse split depends substantially on the reference set. For example, the framework exhibits a larger level share than the main chain, the

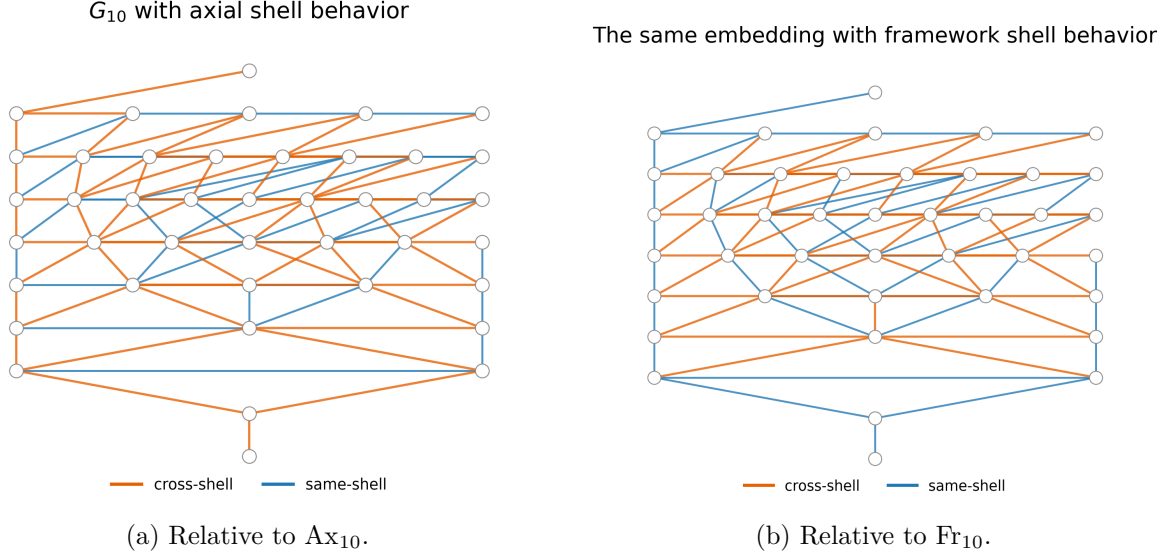


Figure 2: Same-shell and cross-shell edge behavior for two different reference sets. In each panel, blue edges remain inside a shell and orange edges cross between adjacent shells.

n	reference set	level share	transverse share	max shell radius
8	M_n	36.2%	63.8%	3
8	Ax_n	36.2%	63.8%	4
8	Sp_n	34.0%	66.0%	4
8	Fr_n	48.9%	51.1%	2
10	M_n	35.1%	64.9%	4
10	Ax_n	40.4%	59.6%	5
10	Sp_n	40.4%	59.6%	5
10	Fr_n	45.6%	54.4%	3
12	M_n	34.4%	65.6%	6
12	Ax_n	42.3%	57.7%	6
12	Sp_n	40.3%	59.7%	6
12	Fr_n	41.5%	58.5%	4

Table 1: Edgewise directional statistics for the canonical reference sets.

axis, or the spine at $n = 8$ and $n = 10$, while the axial and spinal shell geometries are visually distinguishable in the figures, with the local discrepancies marked explicitly in Figure 1a–1b.

6.2 Combined signatures and directional mixing

Observation 6.2. Directionally mixed edges form a substantial part of G_n throughout the tested range. The mixed-edge share remains between 37.2% and 43.5% for $8 \leq n \leq 12$, and the number of distinct combined signatures increases from 24 at $n = 8$ to 34 at $n = 12$.

Remark 6.3. Observation 6.2 is the most direct empirical reflection of Corollary 5.6. The theorem says that different reference sets cannot induce the same field globally; the computations show that their disagreement is not confined to a small exceptional subset of edges.

6.3 Directional drift of local invariants

For every oriented edge (λ, μ) we computed

$$\Delta \deg = \deg(\mu) - \deg(\lambda), \quad \Delta \dim_{\text{loc}} = \dim_{\text{loc}}(\mu) - \dim_{\text{loc}}(\lambda),$$

n	distinct combined signatures	mixed-edge share	coherent-edge share
8	24	42.6%	57.4%
9	32	41.1%	58.9%
10	32	41.2%	58.8%
11	33	43.5%	56.5%
12	34	37.2%	62.8%

Table 2: Combined directional signatures in the tested range.

directional class	mean Δ deg	median Δ deg	share Δ deg > 0	mean Δ dim _{loc}	share Δ dim _{loc} > 0	mean Δh
axial inward	1.81	2	65.5%	0.34	38.6%	-0.98
spinal inward	2.10	2	71.6%	0.33	35.7%	-0.60
framework inward	-1.23	-1	27.0%	-0.42	3.2%	0.93
axial level	0.00	0	35.0%	0.00	8.7%	0.00
spinal level	0.00	0	34.6%	0.00	12.3%	0.00
framework level	0.00	0	29.6%	0.00	7.3%	0.00

Table 3: Empirical drift of local invariants along selected directional classes, aggregated over $8 \leq n \leq 12$.

together with Δh . Table 3 aggregates these quantities over all oriented edges of the tested range $8 \leq n \leq 12$.

Observation 6.4. The empirical drift of local invariants depends strongly on the directional regime. In the tested range, axial inward and spinal inward motion have positive average drift in both degree and local simplex dimension, while framework inward motion has negative average drift in both quantities. Numerically, the mean degree drift is 1.81 for axial inward edges, 2.10 for spinal inward edges, and -1.23 for framework inward edges.

Remark 6.5. The level classes have zero mean drift by symmetry, but their positive-increment shares remain informative. In particular, the positive degree share is about 35% for axial and spinal level motion, compared with 29.6% for framework level motion on the tested range.

6.4 Corridor profiles

We next pass from individual edges to canonical corridors. Figure 3 shows three corridor types from the same starting vertex in G_{12} .

Table 4 summarizes median hit times for several targets. The columns “to Ax_n ” and “to Sp_n ” measure the median number of corridor steps needed to hit the corresponding reference set. For the complexity-based targets, hit times are computed only over successful starts, while the accompanying success column records the proportion of starts whose canonical corridor reaches the target at all. The column “to top degree” records the median first-hit time for the maximum-degree zone, together with its success rate along the chosen corridor family. The final two columns do the same for the top local-simplex-dimension zone.

Observation 6.6. Canonical corridors toward different reference sets are visibly non-coincident, both geometrically and combinatorially. In particular, framework corridors remain strongly boundary-confined: in Table 4 their success rate for the top-degree zone is below 5% at each of $n = 8, 10, 12$, while axial corridors reach that zone with success rates between 51.9% and 63.6%.

Observation 6.7. In the tested range, corridors directed toward axial and spinal neighborhoods provide more direct access to structured interior regions than framework corridors. This is visible both in Figure 3 and in the corridor statistics: axial and spinal corridors always reach the corresponding central neighborhoods by construction, whereas framework corridors reach top-complexity zones only rarely.

Canonical corridors in G_{12} from (3, 3, 3)

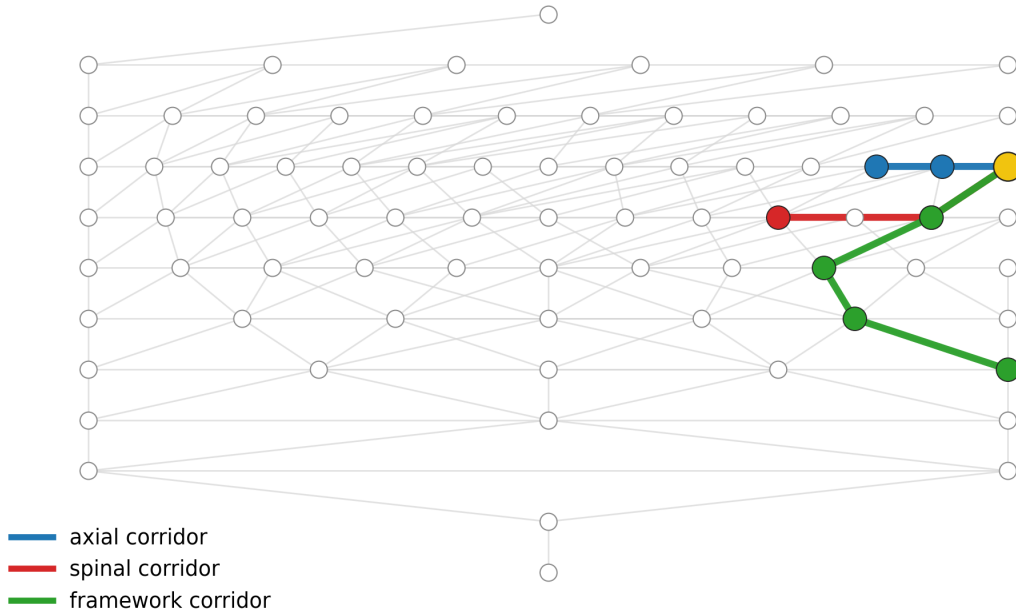


Figure 3: Canonical axial, spinal, and framework corridors from the same starting vertex in G_{12} , defined by the lexicographically minimal descent rule.

n	corridor type	to Ax_n	to Sp_n	to top degree	success	to top simplex	success
8	axial	2	1.5	2	63.6%	1	95.5%
8	spinal	1.5	1	1.5	36.4%	1	95.5%
8	framework	0	0	0	4.5%	0	36.4%
10	axial	2	2	1	57.1%	0	100.0%
10	spinal	1	2	1	31.0%	0	100.0%
10	framework	0.5	0	0	2.4%	0	57.1%
12	axial	2	2	2	51.9%	1	63.6%
12	spinal	2	2	2	22.1%	1	53.2%
12	framework	1	1	0.5	2.6%	0	14.3%

Table 4: Corridor access statistics for selected geometric and complexity targets.

6.5 Summary of empirical anisotropy

The computations support the following qualitative picture. First, the canonical directional fields are visibly non-coincident, both edgewise and pathwise. Second, local complexity drift depends on the directional regime: axial and spinal inward motion tend to move toward higher-complexity regions, while framework inward motion tends to move away from them. Third, access to structured interior regions is directionally uneven: corridor families relative to the axis, the spine, and the framework do not play interchangeable roles.

These observations do not replace the strict theory of Sections 2–5. Rather, they show how that theory manifests itself concretely in finite partition graphs and provide an initial measured atlas of anisotropy in G_n .

7 Conclusion and open problems

We developed a directional formalism for the partition graph G_n based on graph distance from canonical reference sets. This formalism yields inward, outward, and level edge classes, shell decompositions, and monotone inward geodesics, which we interpret as directional corridors. The central structural result is the non-equivalence theorem: distinct nonempty reference sets induce distinct directional fields. Together with the intrinsic acyclic height orientation, this gives a first precise formal meaning to the statement that the partition graph is anisotropic.

A second, conceptual contribution of the paper is the controlled-access principle. It shows that any region known to lie in a bounded neighborhood of the axis, the spine, or the framework automatically inherits corresponding directional corridors. In this way, earlier morphological results can be read in directional terms without being reproved here.

The computational atlas complements the strict theory. It does not prove universal optimality statements, but it shows that the directional language introduced in this paper captures visible and measurable structure already in the tested range of values of n .

We conclude with several open problems.

Problem 7.1 (Quantitative anisotropy). Develop numerical invariants measuring the extent of anisotropy in G_n . Natural candidates include the mixed-edge share, divergences between directional drift profiles, and distances between corridor families associated with different reference sets.

Problem 7.2 (Directional access to complexity). Determine whether high-complexity regions of G_n , such as high-degree zones or top simplex layers, are asymptotically more accessible through certain directional regimes than through others.

Problem 7.3 (Compatibility of directional fields). Study the existence of paths that are simultaneously well behaved with respect to several reference sets. For example, when can a path be spinal-inward while also nonincreasing in axial distance?

Problem 7.4 (Rear-directed geometry). Clarify whether rear-directed transport defines a genuinely new directional field or whether it can be reduced to the existing axis/spine/framework language.

Problem 7.5 (Directional morphology across n). Extend the present fixed- n theory to the comparative-growth picture across n . How do directional fields behave under natural overlays $G_n \rightarrow G_{n+k}$? Which directional patterns stabilize, and which remain local to small or intermediate values of n ?

Problem 7.6 (Toward a discrete transport theory). Develop a broader framework in which directional corridors, shell crossings, and controlled neighborhoods are treated as parts of a discrete transport geometry on G_n .

Acknowledgements

The author acknowledges the use of ChatGPT (OpenAI) for discussion, structural planning, and editorial assistance during the preparation of this manuscript. All mathematical statements, proofs, computations, and final wording were checked and approved by the author, who takes full responsibility for the contents of the paper.

References

- [1] G. E. Andrews, *The Theory of Partitions*, Encyclopedia of Mathematics and its Applications, Vol. 2, Addison–Wesley, Reading, MA, 1976.

- [2] R. P. Stanley, *Enumerative Combinatorics. Vol. 1*, second ed., Cambridge University Press, Cambridge, 2011.
- [3] F. B. Lyudogovskiy, *The homotopy type of the clique complex of the partition graph*, arXiv:2603.14370 [math.CO], 2026. Available at [arXiv:2603.14370](#).
- [4] F. B. Lyudogovskiy, *Local Morphology of the Partition Graph*, arXiv:2603.18696 [math.CO], 2026. Available at [arXiv:2603.18696](#).
- [5] F. B. Lyudogovskiy, *The Partition Graph as a Growing Discrete Geometric Object*, arXiv:2603.21221 [math.CO], 2026. Available at [arXiv:2603.21221](#).
- [6] F. B. Lyudogovskiy, *Axial Morphology of the Partition Graph: Self-Conjugate Axis, Spine, and Concentration*, arXiv:2603.22546 [math.CO], 2026. Available at [arXiv:2603.22546](#).
- [7] F. B. Lyudogovskiy, *Simplex Stratification and Phase Boundaries in the Partition Graph*, arXiv:2603.23228 [math.CO], 2026. Available at [arXiv:2603.23228](#).
- [8] F. B. Lyudogovskiy, *The Degree Landscape of the Partition Graph: Maximal Degree, Extremal Vertices, and Spectra*, arXiv:2603.24141 [math.CO], 2026. Available at [arXiv:2603.24141](#).